

A new parton model for the soft interactions at high energies: two channel approximation.

E. Gotsman,^{1,*} E. Levin,^{1,2,†} and I. Potashnikova^{2,‡}

¹*Department of Particle Physics, School of Physics and Astronomy,
Raymond and Beverly Sackler Faculty of Exact Science, Tel Aviv University, Tel Aviv, 69978, Israel*

²*Departamento de Física, Universidad Técnica Federico Santa María, and Centro Científico-Tecnológico de Valparaíso, Avda. Espana 1680, Casilla 110-V, Valparaíso, Chile*

(Dated: June 12, 2022)

In this paper we achieve a fairly good description of four experimental observables: $\sigma_{\text{tot}}, \sigma_{\text{el}}, B_{\text{el}}$ and the single diffraction cross sections, for proton-proton scattering, in a two channel model for the structure of hadrons at high energy. The impact parameter dependence of the scattering amplitudes show that soft interactions at high energies measured at the LHC, have a much richer structure than presumed.

Our approach has been discussed in a recent paper [1] and it is based (i) on Pomeron calculus in 1+1 space-time, suggested in Ref. [2], and (ii) on simple assumptions of hadron structure, related to the impact parameter dependence of the scattering amplitude. This parton model stems from QCD, assuming that the unknown non-perturbative corrections lead to the fixing of the size of the interacting dipoles. The advantage of this approach is that it satisfies both the t -channel and s -channel unitarity, and can be used for summing all diagrams of the Pomeron interaction, including Pomeron loops. In other words, we can use this approach for all possible reactions: dilute-dilute (hadron-hadron), dilute-dense (hadron-nucleus) and dense-dense (nucleus-nucleus), parton systems scattering. Hence, we present in the paper the first description of the data (for proton-proton scattering) based on a model that satisfies both t and s channel unitarity.

PACS numbers: 12.38.-t, 24.85.+p, 25.75.-q

Introduction.

In our recent paper [1] we proposed a new parton model for high energy soft interactions, which is based on Pomeron calculus in 1+1 space-time dimensions, suggested in Ref. [2], and on simple assumptions of hadron structure, related to the impact parameter dependence of the scattering amplitude. This parton model stems from QCD, assuming that the unknown non-perturbative corrections lead to fixing the size of the interacting dipoles. The advantage of this approach is that it satisfies both the t -channel and s -channel unitarity, and can be used for summing all diagrams of the Pomeron interaction including Pomeron loops. In other words, we can use this approach for all possible reactions: dilute-dilute (hadron-hadron), dilute-dense (hadron-nucleus) and dense-dense (nucleus-nucleus) parton system scattering.

We showed that this model is able to describe high energy data on the total and elastic cross sections for proton-proton scattering, but the simple version of Ref.[1] leads to vanishing of diffractive production. In this letter we propose a two channel model which generates diffraction production in the region of small masses.

The new parton model (generalities).

As we have discussed in Ref.[1, 2] the new parton model is based on three ingredients:

1. The Colour Glass Condensate (GCC) approach (see Ref.[3] for a review), which can be re-written in the equivalent form as the interaction of BFKL Pomerons[4] in a limited range of rapidities ($Y \leq Y_{\text{max}}$):

$$Y \leq \frac{2}{\Delta_{\text{BFKL}}} \ln \left(\frac{1}{\Delta_{\text{BFKL}}^2} \right) \quad (1)$$

where Δ_{BFKL} denotes the intercept of the BFKL Pomeron[5]. In our model $\Delta_{\text{BFKL}} \approx 0.2 - 0.25$ leading to $Y_{\text{max}} = 20 - 30$, which covers all collider energies.

2. The following Hamiltonian:

$$\mathcal{H}_{\text{NPM}} = -\frac{1}{\gamma} \bar{P} P \quad (2)$$

where NPM stands for “new parton model”. P and \bar{P} are the BFKL Pomeron fields. The fact that it is self dual is evident. This Hamiltonian in the limit of small \bar{P} reproduces the Balitsky-Kovchegov Hamiltonian \mathcal{H}_{BK} (see Ref.[2] for details). This condition is the most important one for determining the form of \mathcal{H}_{NPM} . γ in Eq. (2) denotes the dipole-dipole scattering amplitude, which in QCD is proportional to $\bar{\alpha}_S^2$.

3. The new commutation relations:

$$(1 - P)(1 - \bar{P}) = (1 - \gamma)(1 - \bar{P})(1 - P) \quad (3)$$

For small γ and in the regime where P and \bar{P} are also small, we obtain

$$[P, \bar{P}] = -\gamma + \dots \quad (4)$$

consistent with the standard BFKL Pomeron calculus (see Ref.[2] for details) .

In Ref.[2], it was proved that the scattering matrix for the model is given by

$$\begin{aligned} S_{m\bar{n}}^{\text{NPM}}(Y) &= e^{\frac{1}{\gamma} \int_0^Y d\eta [\ln(1-p) \frac{\partial}{\partial \eta} \ln(1-\bar{p}) + \bar{p}p]} [1 - p(Y)]^m [1 - \bar{p}(0)]^{\bar{n}} \Big|_{p(0)=1-e^{-\gamma\bar{n}}; \bar{p}(Y)=1-e^{-\gamma m}} \\ &= [1 - p(Y)]^m e^{\frac{1}{\gamma} \int_0^Y d\eta [\ln(1-\bar{p}) + \bar{p}]} p \end{aligned} \quad (5)$$

where $p(\eta)$ and $\bar{p}(\eta)$ are solutions of the classical equations of motion and have the form:

$$P(\eta) = \frac{\alpha + \beta e^{(1-\alpha)\eta}}{1 + \beta e^{(1-\alpha)\eta}}; \quad \bar{P}(\eta) = \frac{\alpha(1 + \beta e^{(1-\alpha)\eta})}{\alpha + \beta e^{(1-\alpha)\eta}}; \quad (6)$$

where the parameters β and α should be determined from the boundary conditions:

$$P(\eta = 0) = p_0; \quad \bar{P}(\eta = Y) = \frac{\alpha}{P(\eta = Y)} = \bar{p}_0 \quad (7)$$

It is interesting to compare the scattering amplitude given by this expression to that obtained from the BK equation, which describes deep inelastic scattering on nuclei in QCD. For which we have

$$S_{m\bar{n}}^{\text{BK}}(Y) = \int dP(\eta) d\bar{P}(\eta) e^{\frac{1}{\gamma} \int_0^Y d\eta [\ln(1-P) \frac{\partial}{\partial \eta} \ln(1-\bar{P}) - \ln(1-P)PP]} (1 - P(Y))^m (1 - \bar{P}(0))^{\bar{n}} \quad (8)$$

In the classical approximation

$$\begin{aligned} S_{m\bar{n}}^{\text{BK}}(Y) &= e^{\frac{1}{\gamma} \int_0^Y d\eta [\ln(1-p) \frac{\partial}{\partial \eta} \ln(1-\bar{p}) - \ln(1-\bar{p})p]} [1 - p(Y)]^m [1 - \bar{p}(0)]^{\bar{n}} \Big|_{p(0)=1-e^{-\gamma\bar{n}}; \bar{p}(Y)=1-e^{-\gamma m}} \\ &= [1 - p(Y)]^m \end{aligned} \quad (9)$$

Note, that the solution for \bar{P} , is not relevant for the BK amplitude, which is determined entirely by $P(Y)$. On the other hand the scattering amplitude in the NPM depends on \bar{P} . Nevertheless, the two models should be similar in the regime where the BK evolution is valid. The results of the estimates in Ref.[2] shows that in the region close to saturation, the differences between BK and NPM are quite significant.

The new parton model (interrelation with QCD).

As has been mentioned, in the limited range of energies, given by Eq. (1), both QCD and our model describe the interaction of the BFKL Pomerons[5]. For weak fields P and \bar{P} , the model reproduces the BK limit of the CGC approach, assuming that the non-perturbative corrections result from fixing the size of the interacting dipoles, and hence, the successful description of the soft data at high energies in CGC approach [6–13] supports the idea that this effective size is rather small. The model leads to the descriptions that satisfy both t -unitarity and s -channel unitarity, while, as it was shown in Ref.[2], the BFKL Pomeron calculus in the BK limit, as well as the Braun Hamiltonian[14] for dense-dense system scattering violates s -channel unitarity. Unfortunately, we are still far from being able to solve this problem in the effective QCD theory at high energy (i.e. in the CGC /saturation approach).

The new parton model (two channel approximation).

Our model includes three essential ingredients: (i) the new parton model for dipole-dipoles scattering amplitude that has been discussed above; ii) the simplified two channel model that enables us to take into account diffractive production in the low mass region, and (iii) the assumptions for impact parameter dependence of the initial conditions.

Following Good and Walker [20] in the two channel approximation we replace the rich structure of the diffractively produced states, by a single state with the wave function ψ_D . The observed physical hadronic and diffractive states are written in the form

$$\psi_h = \alpha \Psi_1 + \beta \Psi_2; \quad \psi_D = -\beta \Psi_1 + \alpha \Psi_2; \quad \text{where} \quad \alpha^2 + \beta^2 = 1; \quad (10)$$

Functions ψ_1 and ψ_2 form a complete set of orthogonal functions $\{\psi_i\}$ which diagonalize the interaction matrix \mathbf{T}

$$A_{i,k}^{i'k'} = \langle \psi_i \psi_k | \mathbf{T} | \psi_{i'} \psi_{k'} \rangle = A_{i,k} \delta_{i,i'} \delta_{k,k'}. \quad (11)$$

The unitarity constraints take the form

$$2 \text{Im} A_{i,k}(s, b) = |A_{i,k}(s, b)|^2 + G_{i,k}^{in}(s, b), \quad (12)$$

where $G_{i,k}^{in}$ denotes the contribution of all non diffractive inelastic processes, i.e. it is the summed probability for these final states to be produced in the scattering of a state i off a state k . In Eq. (12) $\sqrt{s} = W$ denotes the energy of the colliding hadrons and b denotes the impact parameter. In our approach we used the solution to Eq. (12) given by Eq. (5) and

$$A_{ik} = 1 - S_{ik}^{\text{NPM}}(Y) \quad (13)$$

The general formulae.

Initial conditions: Following Ref.[1] we chose the initial conditions in the form:

$$p_i(b') = p_{0i} S(b', m_i) \quad \text{with} \quad S(b, m_i) = m_i b K_1(m_i b); \quad \bar{p}_i(\mathbf{b} - \mathbf{b}') = p_{0i} S(\mathbf{b} - \mathbf{b}', m_i) \quad z_m = e^{\Delta(1-p_{01})Y} \quad (14)$$

Both p_{0i} and masses m_i , as well as the Pomeron intercept Δ , are fitting parameters of the model. Note, that $S(b, m_i) \xrightarrow{m_i b \gg 1} \exp(-m_i b)$ in accord with the Froissart theorem[15],

From Eq. (14) we find that

$$a_{ik}(b, b') \equiv a_{i,k}(p_i, \bar{p}_k, z_m) = \frac{1}{2} (p_i + \bar{p}_k) + \frac{1}{2 z_m} ((1 - p_i)(1 - \bar{p}_k) - D_{i,k}); \quad (15)$$

$$b_{i,k}(b, b') \equiv b_{i,k}(p_i, \bar{p}_k, z_m) = \frac{1}{2} \frac{p_i - \bar{p}_k}{1 - p_i} - \frac{1}{2 z_m (1 - p_i)} ((1 - p_i)(1 - \bar{p}_k) - D_{i,k}); \quad (16)$$

$$D_{i,k} = \sqrt{4 p_i (1 - p_i) (1 - \bar{p}_k) z_m - ((1 - p_i)(1 - \bar{p}_k) - (p_i - \bar{p}_k) z_m)^2}; \quad (17)$$

These equation are the explicit solutions to Eq. (6) and Eq. (7).

Amplitudes: In the following equations $p_i \equiv p_i(b')$ and $\bar{p}_k \equiv \bar{p}_k(\mathbf{b} - \mathbf{b}')$.

$$z = e^{\Delta(1-p_{01})Y}$$

$$S_{ik}(a_{ik}, b_{ik}, z) \equiv S(a_{ik}(b, b'), b_{ik}(b, b'), z_m), \quad X_{i,k}(a, b, z) \equiv X(a_{ik}(b, b'), b_{ik}(b, b'), z_m)$$

$$X(a_{ik}, b_{ik}, z) = \frac{a_{ik} + b_{ik} z}{1 + b_{ik} z} \quad (18)$$

$$\begin{aligned} SS_{ik}(a_{ik}, b_{ik}, z) = & \\ & -(a_{ik} - 1) \text{Li}_2(-b_{ik} z) + a_{ik} \text{Li}_2\left(-\frac{b_{ik} z}{a_{ik}}\right) + (a_{ik} - 1) \text{Li}_2\left(\frac{a_{ik} + b_{ik} z}{a_{ik} - 1}\right) + \frac{1}{2} a_{ik} \log^2((1 - a_{ik}) b_{ik} z) \\ & -(a_{ik} - 1) \log(b_{ik} z + 1) \log((1 - a_{ik}) b_{ik} z) - \left(a_{ik} \log(z) - (a_{ik} - 1) \log\left(-\frac{b_{ik} z + 1}{a_{ik} - 1}\right)\right) \log(a_{ik} + b_{ik} z) \\ & + a_{ik} \log(z) \log\left(\frac{b_{ik} z}{a_{ik}} + 1\right) \end{aligned} \quad (19)$$

$$S_{ik}(a_{ik}, b_{ik}, z) = SS_{ik}(a_{ik}, b_{ik}, z) - SS_{ik}(a_{ik}, b_{ik}, z = 1) \quad (20)$$

The amplitude is equal to

$$A_{ik}(S, b) = 1 - \exp \left(\frac{1}{p_{01}} \int \frac{m_1^2 d^2 b'}{4\pi} \left(S_{ik}(a_{ik}, b_{ik}, z_m) + a_{ik}(b, b') \Delta (1 - p_0) Y \right) - \int \frac{m_1^2 d^2 b'}{4\pi} \bar{p}_k(\mathbf{b} - \mathbf{b}', m_k) X(a_{ik}, b_{ik}, z_m) \right) \quad (21)$$

Observables: The physical observables in this model can be written as follows

$$\text{elastic amplitude : } a_{el}(s,) = i (\alpha^4 A_{1,1} + 2\alpha^2 \beta^2 A_{1,2} + \beta^4 A_{2,2}); \quad (22)$$

$$\text{elastic cross section : } \sigma_{tot} = 2 \int d^2 b a_{el}(s, b); \quad \sigma_{el} = \int d^2 b |a_{el}(s, b)|^2;$$

$$\text{elastic slope : } B_{el} = \frac{1}{2} \frac{\int b^2 d^2 b \text{Im} A_{el}(Y, b)}{\int d^2 b \text{Im} A_{el}(Y, b)}; \quad (23)$$

$$\text{optical theorem : } 2 \text{Im} A_{i,k}(s, t=0) = 2 \int d^2 b \text{Im} A_{i,k}(s, b) = \sigma_{el} + \sigma_{in} = \sigma_{tot}; \quad (24)$$

$$\text{single diffraction : } \sigma_{sd}^{GW} = \int d^2 b (\alpha \beta \{-\alpha^2 A_{1,1} + (\alpha^2 - \beta^2) A_{1,2} + \beta^2 A_{2,2}\})^2; \quad (25)$$

$$\text{double diffraction : } \sigma_{dd}^{GW} = \int d^2 b \alpha^4 \beta^4 \{A_{1,1} - 2 A_{1,2} + A_{2,2}\}^2. \quad (26)$$

Comparison with experimental data for proton-proton scattering.

As we have seen in the previous section, we introduce three dimensionless parameters: Δ - the intercept of the BFKL Pomeron, and p_{01} (p_{02}) - the amplitudes of the dipole-dipole scattering at low energies, and β which is related to the contribution of the diffractive production. For b -dependence we suggested a specific form (see Eq. (14)) which is characterized by the dimensional parameters: m_i . These parameters are determined by fitting to the experimental data. We choose to describe five observables: total and elastic cross sections, the elastic slope and single and double diffractions at low masses (see Eq. (22)-Eq. (26)).

The situation with the experimental data on the single and double diffraction production in proton-proton scattering at high energies, is far from clear. It was well summarized in Ref.[19], to which we refer the reader. We assume that the two channel model is able to describe proton-proton diffraction production in the entire kinematic region of produced mass. As is shown in Ref.[21] for $\Delta > 0$ the integral over the produced mass in diffraction is convergent, and the Good-Walker mechanism[20] is able to describe the diffraction production both of small and large masses. However, the simple two channel model is a simplification, but we hope to learn something by attempting to fit all available data using this simple model.

From Fig. 1 one can see that we can describe the data for $W \geq 0.5 \text{ TeV}$. The values of parameters of the fit are shown in Table I. The two sets have quite different values of m_1 and m_2 . However, note that the set of parameters I in Table I does not describe σ_{el} well, having the better value of $\chi^2/\text{d.o.f.}$ This fact means that the set I produces a better fit to the diffractive data.

Comparing these parameters with the resulting curves in Fig. 1 we see that the shadowing corrections play an essential role. First, we note that the value of $\Delta_{\text{dressed}} = \Delta(1 - p_{01})$ is rather large (about 0.5) in all variants. Recall, that means that $\Delta \approx 1$. Factor $(1 - p_{01})$ in Δ_{dressed} , stems from the enhanced diagrams that contribute to the Green function of the Pomeron. The resulting $\sigma_{tot} \propto s^{\Delta_{\text{eff}}}$ with $\Delta_{\text{eff}} \approx 0.07$. Such a reduction from Δ_{dressed} to Δ_{eff} occurs due to the strong shadowing corrections.

As one can see from Fig. 2-a we describe the single diffraction production data, which has been taken from Ref.[22] and are shown in Fig. 2-b. One can see that the TOTEM value of the single diffraction cross section is 9.1 ± 2.9 (see Ref.[22]), while our estimates lead to $\sigma_{sd}^{\text{md}} = 12 - 13 \text{ mb}$. As you can see from Fig. 2-a and Fig. 2-b, our model leads to values of the single diffraction cross section, which are close to our predictions from the CGC motivated model of Ref.[9] (the curve GLM in Fig. 2-b). We refer the reader to Ref.[19] in which the situation with tensions between different experimental groups on the single diffraction cross section has been discussed.

One can see from the Table II and from Fig. 3-a, that we are able to describe only half of the double diffractive cross section. This reflects the situation which we had in our previous attempts to describe this process[9]. As one can see from the Table II and Fig. 3-a we reproduce the energy behaviour of the experimental data on the double diffraction but cannot obtain the large value of the cross section at $W = 0.5 \text{ TeV}$. The same problem is faced by the other groups (see, for example, Ref.[19] and reference therein). In Fig. 3-a we plot our prediction to which we add the constant cross section to fit data at $W = 0.5 \text{ TeV}$. With this parameter, we describe the data. Concluding, we think

that a good description of the double diffraction data will be achieved in future by developing a more complicated model for the hadron structure and accumulating more and better experimental data.

Variant of the fit	Δ_{dressed}	p_{01}	p_{02}	m_1 (GeV)	m_2 (GeV)	β^2	$\chi^2/\text{d.o.f}$
I	0.48 ± 0.01	0.72 ± 0.05	0.006 ± 0.001	1.033 ± 0.01	0.50 ± 0.09	0.25 ± 0.01	1.1
II	0.52 ± 0.01	0.644 ± 0.02	0.10 ± 0.01	1.04 ± 0.01	1.79 ± 0.02	0.32 ± 0.01	1.1

TABLE I: Fitted parameters. $\Delta_{\text{dressed}} = \Delta(1 - p_{01})$.

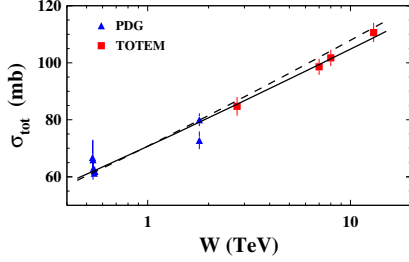


Fig. 1-a

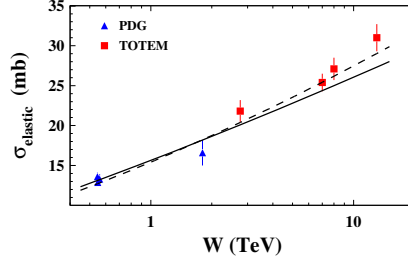


Fig. 1-b

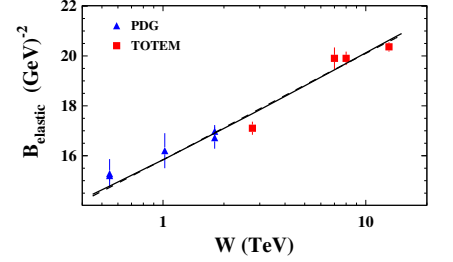


Fig. 1-c

FIG. 1: The energy behaviour of σ_{tot} , σ_{el} and the slope B_{el} for proton-proton scattering in our model. The solid line describes the variant I in Table I while the dashed line corresponds to variant II. Data are taken from Refs.[17, 18].

Dependence on impact parameters

In Fig. 4 we plot the scattering amplitudes as a function of the impact parameter b . One can see that the two channel model generates very interesting and unexpected structure. One amplitude $A_{11}(b)$ has reached the unitarity limit $A_{11}(b=0) = 1$ at $W = 0.5 \text{ TeV}$ and shows the increasing of the radius of the interaction with energy. The two other amplitudes are far from the unitarity limit even at ultra high energy $W = 99 \text{ TeV}$. They increase as $W^{\Delta_{\text{eff}}}$ with $\Delta_{\text{eff}} \sim 0.1$. The behaviour as a function of b is also unexpected. Both A_{11} and A_{22} decrease monotonically at large b , while A_{12} has a maximum which moves to larger values of b , and the value of the amplitude for this maximum increases as $W^{\Delta_{\text{eff}}}$. On the other hand, $A_{12}(b=0)$ is almost independent on W .

Such dependence of the amplitudes generate the elastic amplitude which is smaller than the unitarity limit even at very high energies (see Fig. 4-a). This conclusion is in accord with the recent paper of Ref.[24] in which it is demonstrated that in the Miettinen-Pumplin [25] approach the elastic amplitude $A_{el}(b=0) \approx 0.92 < 1$ at $W = 57 \text{ TeV}$. Note, that this approach is ideologically close to ours and second, that in Ref.[24] the entire set of soft interaction data has been described successfully.

In Fig. 2-a we present the comparison between the elastic amplitude in our 2 channel model and in one channel model of Ref. [1]. One can see that these two amplitudes have a different behaviour as a function of energy and

W (TeV)	σ_{tot} (mb)	σ_{el} (mb)	B_{el} (GeV^{-2})	σ_{sd} (mb)	σ_{dd} (mb)
0.55	61.86(61.59)	13.1(12.64)	14.78(14.80)	6.99(7.4)	1.1(1.41)
1.8	79.16(80.271)	18.178(18.14)	15.872(16.95)	9.55(10.14)	1.47(1.82)
2.76	85.4(87.08)	20.082(20.29)	17.686(17.73)	10.476(11.12)	1.63(1.95)
7	99.37(102.29)	24.37(25.32)	19.44(19.39)	12.464(13.14)	1.98(2.16)
8	101.4(104.5)	25.0(26.07)	19.695(19.62)	12.744 (13.4)	2.03(2.19)
13	108.811(112.61)	27.3(28.90)	20.623(20.46)	13.743 (14.40)	2.12(2.36)

TABLE II: The values of observables in our model for the set of parameters I. In parenthesis the values for the set II.

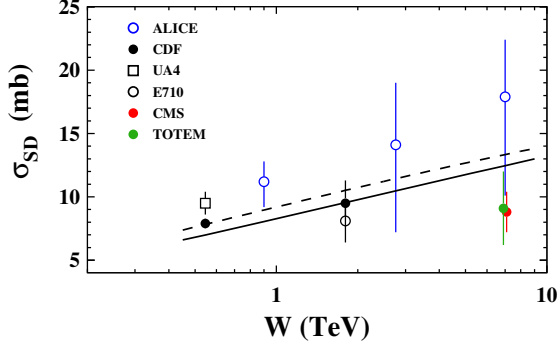


Fig. 2-a

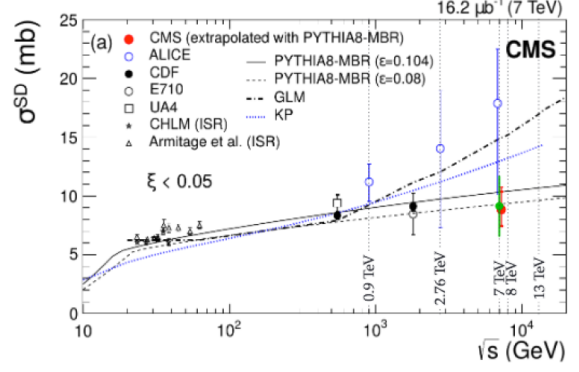


Fig. 2-b

FIG. 2: The single diffraction cross section as function of energy $W = \sqrt{s}$: our description of the data with $W \geq 0.5 \text{ TeV}$ (Fig. 2-a) and the experimental data from Ref.[22] (Fig. 2-b). The data of all experimental groups were extrapolated to the region $M^2 \leq 0.05 s$ using the Pythia Monte-Carlo programs as is shown in Fig. 2-b. M is the mass of hadron produced in single diffraction. The data in Fig. 2-a are taken from Ref.[22] and we refer to this paper (especially to Ref.[9] in it). The curves in Fig. 2-b marked as GLM are taken from Ref.[9] and that as KP is from Ref.[23].

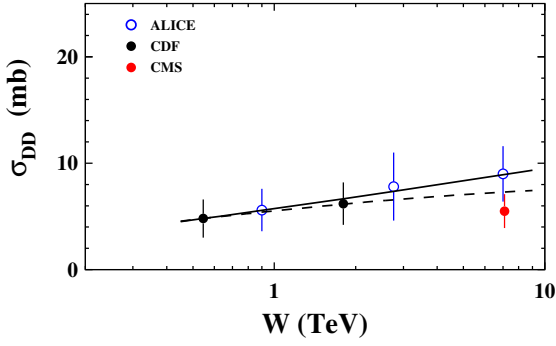


Fig. 3-a

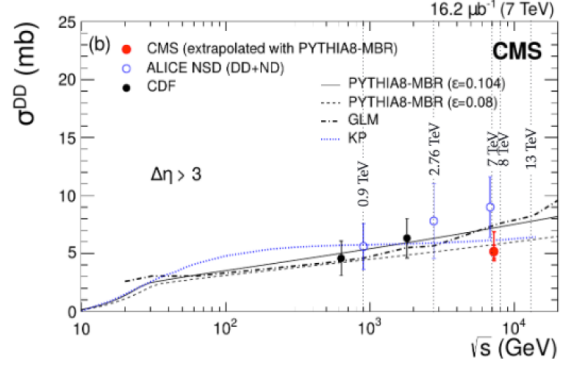


Fig. 3-b

FIG. 3: The double diffraction cross section as function of energy $W = \sqrt{s}$: our description (see text), solid and dashed lines correspond sets I and II of Table I (Fig. 3-a) the experimental points, were taken from Ref.[22]. The notation of the curves are the same as in Fig. 2.

impact parameter. We believe that this figure demonstrates that the modeling of the non-perturbative structure of the hadron is very important in understanding high energy scattering. Fig. 2-b shows the behaviour of $d\sigma_{sd}/db^2$ (see Eq. (25))

$$\frac{d\sigma_{sd}}{db^2} = \left(\alpha\beta \{ -\alpha^2 A_{1,1} + (\alpha^2 - \beta^2) A_{1,2} + \beta^2 A_{2,2} \} \right)^2 \quad (27)$$

One can see that this observable decreases very slowly with energy, and does not show a maximum at large b . Such behaviour is quite different from what we obtain in CGC motivated model (see Ref.[9] Fig.7) and from the estimates of Ref.[24].

Bearing in mind that we describe the experimental data fairly well, we believe that the impact parameter and energy behaviours shown in Fig. 4 and in Fig. 2, illustrate the fact that the soft interaction at high energies could have a much richer structure than we previously assumed.

CONCLUSIONS.

In this paper we showed that the experimental data for proton-proton scattering at high energies can be described in the framework of the new parton model. The model is based on Pomeron calculus in 1+1 space-time, suggested in

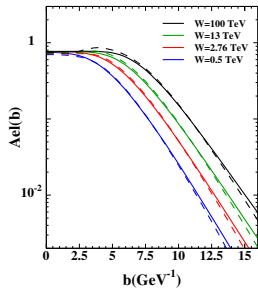


Fig. 4-a

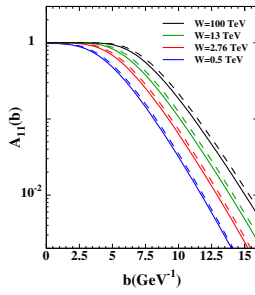


Fig. 4-b

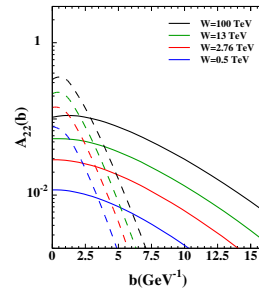


Fig. 4-c

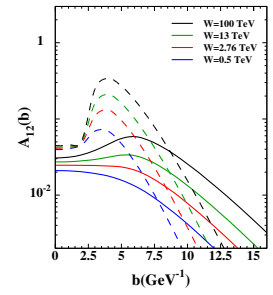


Fig. 4-d

FIG. 4: The scattering amplitudes versus impact parameter b for different energies: Fig. 4-a A_{el} ; Fig. 4-b A_{11} , Fig. 4-c A_{22} , Fig. 4-d A_{12} .

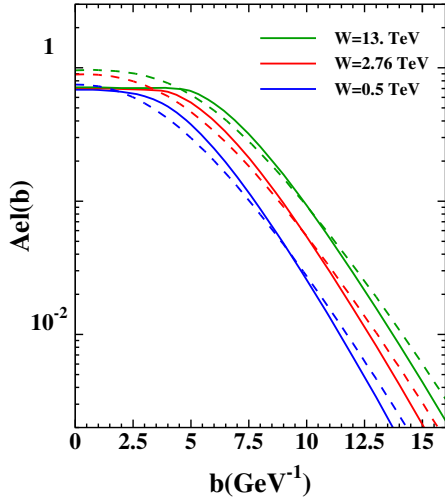


Fig. 5-a

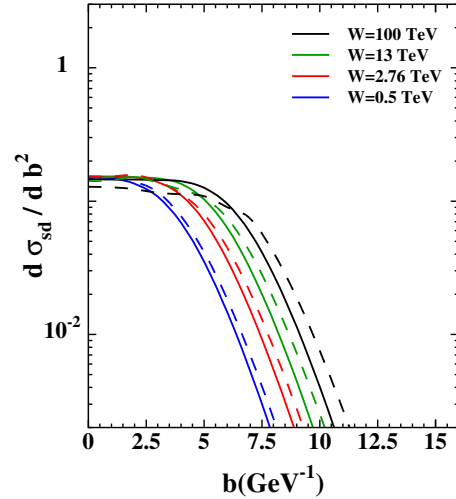


Fig. 5-b

FIG. 5: The scattering amplitudes versus impact parameter b for different energies: Fig. 2-a: the elastic amplitudes for the one channel model of Ref.[1] (dashed line) and for two channel model of this paper (solid line). For estimates in our model we used set I of parameters in Table I; Fig. 2-b : $\frac{d\sigma_{sd}}{db^2}$ of Eq. (27) for the variant two (solid line) and variant one (dashed line) set of parameters.

Ref. [4], and on the simple assumptions on the hadron structure, related to the impact parameter dependence of the scattering amplitude. This parton model stems from QCD, assuming that the unknown non-perturbative corrections lead to fixing the size of the interacting dipoles. The advantage of this approach is that it satisfies both t -channel and s -channel unitarity, and it can be used for summing all diagrams of the Pomeron interaction including the Pomeron loops. In other words, we can use this approach for all possible reactions: dilute-dilute (hadron-hadron), dilute-dense (hadron - nucleus) and dense-dense (nucleus-nucleus) parton system scattering. Unfortunately, we are far from solving this problem in the QCD effective theory at high energy (CGC /saturation approach).

We achieved a fairly good description of three experimental observables: $\sigma_{tot}, \sigma_{el}$ and B_{el} , especially as related to the energy dependence of these observables. We consider a success of the model, that we are able to describe the data on the single diffractive production in the two channel model.

The impact parameter dependance of the scattering amplitudes (see Fig. 4) shows that the soft interaction at high energies measured at the LHC have a much richer structure that we presumed in the past. We believe that we have demonstrated that the character of high energy scattering is closely related to the structure of hadron, which presently is described by a simple two channel model.

A topic for future study, is whether the characteristic behaviour of the $A_{i,k}(b)$ amplitudes as a function of b stems from the first model, that satisfies both s and t channel unitarity, or is the artifact of the simple two channel approach.

We are aware that our model is very naive in describing the hadron structure, but hope that further progress

in accumulating data on diffraction production, as well as the unsolved problem of treating the processes of the multiparticle generation in the framework of our approach, will generate a self consistent picture for high energy scattering at long distances.

Acknowledgements.

We thank our colleagues at Tel Aviv University and UTFSM for encouraging discussions. This research was supported by CONICYT PIA/BASAL FB0821(Chile) and Fondecyt (Chile) grants 1170319 and 1180118 .

* Electronic address: gotsman@post.tau.ac.il

† Electronic address: leving@post.tau.ac.il, eugeniy.levin@usm.cl

‡ Electronic address: irina.potashnikova@usm.cl

- [1] E. Gotsman, E. Levin and I. Potashnikova, “A new parton model for the soft interactions at high energies,” Eur. Phys. J. C **79** (2019) no.3, 192, [arXiv:1812.09040 [hep-ph]].
- [2] A. Kovner, E. Levin and M. Lublinsky, “QCD unitarity constraints on Reggeon Field Theory,” JHEP **1608** (2016) 031, [arXiv:1605.03251 [hep-ph]].
- [3] Y. V. Kovchegov and E. Levin *Quantum chromodynamics at high energy* Vol. 33 (Cambridge University Press, 2012).
- [4] T. Altinoluk, A. Kovner, E. Levin and M. Lublinsky, “Reggeon Field Theory for Large Pomeron Loops,” JHEP **1404** (2014) 075 [arXiv:1401.7431 [hep-ph]].
- [5] V. S. Fadin, E. A. Kuraev and L. N. Lipatov, “On the pomeron singularity in asymptotically free theories”, Phys. Lett. **B60**, 50 (1975); E. A. Kuraev, L. N. Lipatov and V. S. Fadin, “The Pomeron singularity in Nonabelian Gauge Theories” Sov. Phys. JETP **45**, 199 (1977), [Zh. Eksp. Teor. Fiz.72,377(1977)]; I. I. Balitsky and L. N. Lipatov, “The Pomeron singularity in Quantum Chromodynamics,” Sov. J. Nucl. Phys. **28**, 822 (1978), [Yad. Fiz.28,1597(1978)].
- [6] E. Gotsman, E. Levin and I. Potashnikova, “CGC/saturation approach: soft interaction at the LHC energies,” Phys. Lett. B **781** (2018) 155, [arXiv:1712.06992 [hep-ph]].
- [7] E. Gotsman, E. Levin and I. Potashnikova, “A CGC/saturation approach for angular correlations in proton - proton scattering,” Eur. Phys. J. C **77** (2017) no.9, 632, [arXiv:1706.07617 [hep-ph]].
- [8] E. Gotsman, E. Levin and U. Maor, “A model for strong interactions at high energy based on the CGC/saturation approach,” Eur. Phys. J. C **75** (2015) 1, 18 [arXiv:1408.3811 [hep-ph]].
- [9] E. Gotsman, E. Levin and U. Maor, “CGC/saturation approach for soft interactions at high energy: a two channel model,” Eur. Phys. J. C **75** (2015) 5, 179 [arXiv:1502.05202 [hep-ph]].
- [10] E. Gotsman, E. Levin and U. Maor, “CGC/saturation approach for soft interactions at high energy: inclusive production,” Phys. Lett. B **746** (2015) 154 [arXiv:1503.04294 [hep-ph]].
- [11] E. Gotsman, E. Levin and U. Maor, “CGC/saturation approach for soft interactions at high energy: long range correlations,” Eur. Phys. J. C **75** (2015) 11, 518 [arXiv:1508.04236 [hep-ph]].
- [12] E. Gotsman, E. Levin and U. Maor, “CGC/saturation approach for soft interactions at high energy: survival probability of central exclusive production,” Eur. Phys. J. C **76** (2016) no.4, 177, [arXiv:1510.07249 [hep-ph]].
- [13] E. Gotsman, E. Levin, U. Maor and S. Tapia, “CGC/saturation approach for high energy soft interactions: v_2 in proton-proton collisions,” Phys. Rev. D **93** (2016) no.7, 074029, [arXiv:1603.02143 [hep-ph]].
- [14] M. A. Braun, “Nucleus-nucleus scattering in perturbative QCD with $N_c \rightarrow \infty$ Phys. Lett. B **483**, 115 (2000); e-Print Archive:[hep-ph/0003004]; “Nucleus nucleus interaction in the perturbative QCD,” Eur. Phys. J. C **33**, 113 (2004) e-Print Archive: [hep-ph/0309293]; “Conformal invariant pomeron interaction in the perturbative QCD with large N_c ,” Phys. Lett. B **632**, 297 (2006)
- [15] M. Froissart, “Asymptotic Behavior and Subtractions in the Mandelstam Representation”, Phys. Rev. **123** (1961) 1053; A. Martin, “Scattering Theory: Unitarity, Analyticity and Crossing.” Lecture Notes in Physics, Springer-Verlag, Berlin-Heidelberg-New-York, 1969.
- [16] I. Gradshteyn and I. Ryzhik, *Table of Integrals, Series, and Products*, Fifth Edition, Academic Press, London, 1994.
- [17] The Review of Particle Physics (2018), M. Tanabashi et al. (Particle Data Group), Phys. Rev. D **98**, 030001 (2018).
- [18] G. Antchev et al. [TOTEM Collaboration], “First measurement of elastic, inelastic and total cross-section at $\sqrt{s} = 13$ TeV by TOTEM and overview of cross-section data at LHC energies,” CERN-EP-2017-321, CERN-EP-2017-321-V2 arXiv:1712.06153 [hep-ex]; “First determination of the ρ parameter at $\sqrt{s} = 13$ TeV probing the existence of a colourless three-gluon bound state,” CERN-EP-2017-335, Submitted to: Phys.Rev..
- [19] V. A. Khoze, A. D. Martin and M. G. Ryskin, “Elastic and diffractive scattering at the LHC,” Phys. Lett. B **784**, 192 (2018) doi:10.1016/j.physletb.2018.07.054 [arXiv:1806.05970 [hep-ph]].
- [20] M. L. Good and W. D. Walker, “Diffraction Dissociation of Beam Particles”, Phys. Rev. **120** (1960) 1857.
- [21] G. Gustafson, “The Relation between the Good-Walker and Triple-Regge Formalisms for Diffractive Excitation,” Phys. Lett. B **718** (2013) 1054, [arXiv:1206.1733 [hep-ph]].
- [22] Jan Kaspar, “Soft diffraction at LHC”, EPJ Web of Conference **72**, 06005(2018), <https://doi.org/10.1051/epjconf/2018172060005>.
- [23] A. B. Kaidalov and M. G. Poghosyan, “Predictions of Quark-Gluon String Model for pp at LHC,” Eur. Phys. J. C **67** (2010) 397 doi:10.1140/epjc/s10052-010-1301-y [arXiv:0910.2050 [hep-ph]]; “Description of soft diffraction in the framework of reggeon calculus: Predictions for LHC,” arXiv:0909.5156 [hep-ph], talk given at 13th International Conference on Elastic

and Diffractive Scattering (Blois Workshop): “*Moving Forward into the LHC Era (EDS 09)*”.

- [24] V. P. Gonsalves, R. P. da Silva and P. V. R. G. Silva, “*Diffractive excitation in pp and pA collisions at high energies*,” Phys. Rev. D **100** (2019) no.1, 014019 doi:10.1103/PhysRevD.100.014019 [arXiv:1905.00806 [hep-ph]].
- [25] H. I. Miettinen and J. Pumplin, “*Diffraction Scattering and the Parton Structure of Hadrons*,” Phys. Rev. D **18** (1978) 1696. doi:10.1103/PhysRevD.18.1696